On Validation of Fully Coupled Behavior of Porous Media using Centrifuge Test Results

Panagiota Tasiopoulou
PhD Student, National Technical University of Athens, Athens, Greece

Mahdi Taiebat
Associate Professor, Department of Civil Engineering, The University of British Columbia, Vancouver

Nima Tafazzoli
Geotechnical Engineer, Tetra Tech EBA, Vancouver, BC, Canada

Boris Jeremić[1]
Professor, Department of Civil and Environmental Engineering, University of California, Davis, CA, and Faculty Scientist, Earth Science Division, Lawrence Berkeley National Laboratory, Berkeley, CA.

keywords: verification and validation, finite elements, fully coupled analysis, porous media

Abstract

Modeling and simulation of mechanical response of infrastructure object, solids and structures, relies on the use of computational models to foretell the state of a physical system under conditions for which such computational model has not been validated. Verification and Validation (V&V) procedures are the primary means of assessing accuracy, building confidence and credibility in modeling and computational simulations of behavior of those infrastructure objects. Validation is the process of determining a degree to which a model is an accurate representation of the real world from the perspective of the intended uses of the model. It is mainly a physics issue and provides evidence that the correct model is solved (Oberkampf et al., 2002).

Our primary interest is in modeling and simulating behavior of porous particulate media that is fully saturated with pore fluid, including cyclic mobility and liquefaction. Fully saturated soils undergoing dynamic shaking fall in this category. Verification modeling and simulation of fully saturated porous soils is addressed in more detail by (Tasiopoulou et al., 2014), and in this paper we address validation. A set of centrifuge experiments is used for this purpose. Discussion is provided assessing the effects of scaling laws on centrifuge experiments and their influence on the validation. Available validation test are reviewed in view of first and second order phenomena and their importance to validation. For example, dynamics behavior of the system, following the dynamic time, and dissipation of the pore fluid pressures, following diffusion time, are not happening in the same time scale and those discrepancies are discussed. Laboratory tests, performed on soil that is used in centrifuge experiments, were used to calibrate material models that are then used in a validation process. Number of physical and numerical examples are used for validation and to illustrate presented discussion. In particular, it is shown that for the most part, numerical prediction of behavior, using laboratory test data to calibrate soil material model, prior to centrifuge experiments, can be validated using scaled tests. There are, of course, discrepancies, sources of which are analyzed and discussed.

[1]Corresponding Author, Department of Civil and Environmental Engineering, University of California, One Shields Ave, Davis, CA, 95616. jeremic@ucdavis.edu

1 Introduction

Numerical predictions of behavior of civil engineering solids and structures has gained a significant popularity in last decades, particularly with the availability of fast digital computers and a number of commercial and research programs (numerical modeling and simulations tools) that feature nice graphical user interfaces (GUIs). While expansion of use of numerical prediction tools brings great promises for improved design (improved safety and economy) there also exists a danger of using numerical prediction tools for modeling and simulating phenomena for which these tools have not been verified and validated.

Verification and Validation (V&V) procedures are the primary means of assessing accuracy, building confidence and credibility in modeling and computational simulations. Verification is the process of determining that a model implementation accurately represents the developer's conceptual description and specification. It is mainly a mathematics issue, and provides evidence that the model is solved correctly. Validation is the process of determining a degree to which a model is an accurate representation of the real world from the perspective of the intended uses of the model. It is mainly a physics issue and provides evidence that the correct model is solved (Oberkampf et al., 2002).

Verification and validation has recently gained increased attention, with the understanding that numerical prediction results can only be trusted if proper verification and validation has been performed (Mróz, 1988; Arulanandan and Scott, 1993; Zienkiewicz et al., 1994; Roache, 1998; Oberkampf et al., 2002; Oden et al., 2005; Babuška and Oden, 2004; Oden et al., 2010a,b; Oberkampf and Roy, 2010; Bielak et al., 2010; Roy and Oberkampf, 2011).

In this paper, we address the issue of validating the modeling of fully coupled behavior of particular materials (granular soil) using scaled models under increased gravity, so called centrifuge modeling. Basics of validation procedures are presented in Section 2. Detailed discussion on scaling laws, as they apply to our examples, centrifuge tests, and validation results with comments are presented in Section 3. Details of the u-p-U formulation are given by Tasiopoulou et al. (2014) and will not be repeated here. In addition, validation of the elastic-plastic material model used was presented by Jeremić et al. (2008) and will not be covered here either.

2 Validation Procedures

Validation procedures are used to provide evidence that numerical analyst have chosen the right models for modeling phenomena in question. As such, validation procedures are tightly coupled to the physics (mechanics) of the problem. Validation procedures give us information about how much we can trust the numerical simulation results.

The role of validation is graphically shown in Figure 1. It is important to note that both verification and validation procedures are necessary in order to gain confidence in numerical modeling results, and to be able to make informed decisions about the behavior of a problem being analyzed. It is also important to note that real physical behavior of a mechanical system is never fully known. This is a result of a macro scale interpretation of the Heisenberg uncertainty principle (Heisenberg, 1927), stating that one cannot obtain position and momentum of a material particles at the same time resulting from some deterministic or stochastic loading. Hence, only an approximate knowledge (with some level of certainty) of behavior of an object (solid and/or structure), can be gained. This argument emphasizes the need for stochastic treatment of both physical and numerical modeling and simulations (Oberkampf et al., 2002).

A more detailed analysis of validation reveals the importance of a hierarchy of experimental data. Figure 2 shows relationship of real world behavior with verification and (emphasis on) validation. As noted by Oberkampf et al. (2002), validation can be understood as a process to determine how accurately

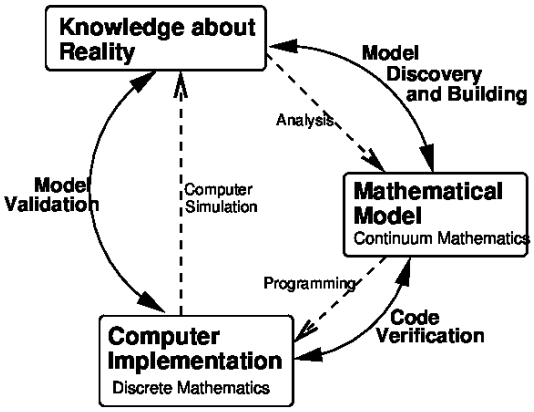

Figure 1: Role of Verification and Validation in relation to the knowledge about reality (graphics inspired by Oberkampf et al. (2002)).

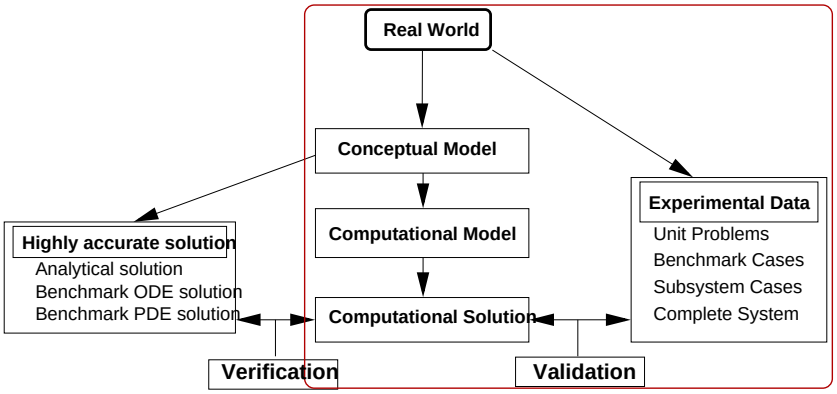

Figure 2: Relationship of verification and validation to the real world, with emphasis on validation and experimental data (inspired by Oberkampf et al. (2002)).

the model (focusing on its intended use) represents the real world, The validation experiments[2] used for this purpose are designed and performed to estimate computational model's ability to model defined physical behavior/phenomena. In a sense, the numerical modeling tool (computational simulation tool) becomes the main customer of designed validation experiment. Ideally, a validation experiments should be jointly designed and performed by physical modeler (experimentalist) and numerical modeler (numerical analyst). Validation experiment should be able to capture relevant/important physics, where physical effects of primary importance are properly modeled while secondary effects might be modeled using some level of approximation.

It is important to note that the validation domain is almost always exclusive of the application domain. That is, real physical phenomena that we are interested in, cannot be fully physically modeled due to complexity, cost, size, etc. For example, civil engineering systems like bridges, buildings, port facilities, dams, nuclear power plants, etc. are to complex, expensive and large to be tested for all loading scenarios of interest. Even if the engineering system is small (less expensive, complex), environmental influences (generalized loads, conditions, wear and tear) are hard to model physically. Validation domain thus represents a simplification of application domain. Figure 3 shows a relationship of validation and application domain for civil engineering applications (structural and soil mechanics) that are almost always exclusively non-overlapping in their systems parameters and system complexity. The inference

[2]As opposed to traditional experiments which are used to improve (a) understanding of physics and (b) mathematical models of/for a phenomena in question.

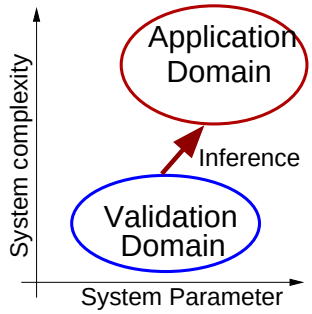

Figure 3: Relationship of the validation domain to the application domain, which, in general for civil engineering application (structural and soil mechanics) are exclusively non-overlapping (Oberkampf et al., 2002)).

from validation to application domain is done numerically. Such inference is based on physics while uncertainties in material behavior, loads, geometry, etc. have to be addressed as well. The importance of uncertainty quantification in experiments and numerical predictions cannot be overstated. All relevant sources of uncertainty in physical models need to be identified and uncertainties estimated. Those uncertainties then need to be propagated through modeling and simulation process.

3 Validation of Coupled Behavior Modeling

3.1 Scaling Laws

Scaling laws are of great importance, not only for the centrifuge modeling itself, but also for the accurate numerical reproduction of the centrifuge tests. The important scaling laws for higher gravity modeling of liquefaction are concerning the dynamic time and the permeability and consequently the diffusion time. The Darcy permeability of the centrifuge model (under increased gravity field of $N \times g$) is N times larger than permeability that was measured in the laboratory (under gravity field of $1 \times g$). This leads to a difference between the scaling factors for the dynamic time and the diffusion time if the same materials (water and soil) are used in the model and prototype. This conflict in time scales is essential to scaling the centrifuge measurements up to the prototype scale since both generation of excess pore fluid pressures (dynamic time) and dissipation of excess pore fluid pressure (diffusion time) happen at the same time throughout shaking and are equally important to the modeling (physical and/or numerical) of liquefaction.

In order to analyze the appropriate scaling of the permeability and the diffusion time, we consider three different cases: A, B and C, as illustrated in Figure 4. It is assumed that water fills the voids of the soil in all cases.

Case A is the object in prototype (original) scale representing the original soil conditions,

Case B is the centrifuge model in model scale, and

Case C is the scaled up prototype model derived from scaling the centrifuge model up to prototype scale.

In literature, the term "prototype model" is sometimes confusingly used to characterize either Case A or Case C, without further clarifications. Herein, Case A is characterized as "Original Model" and Case C as "Prototype Model". Scaling factors for all the important quantities related to our study are presented in Table 1 (Wood, 2004).

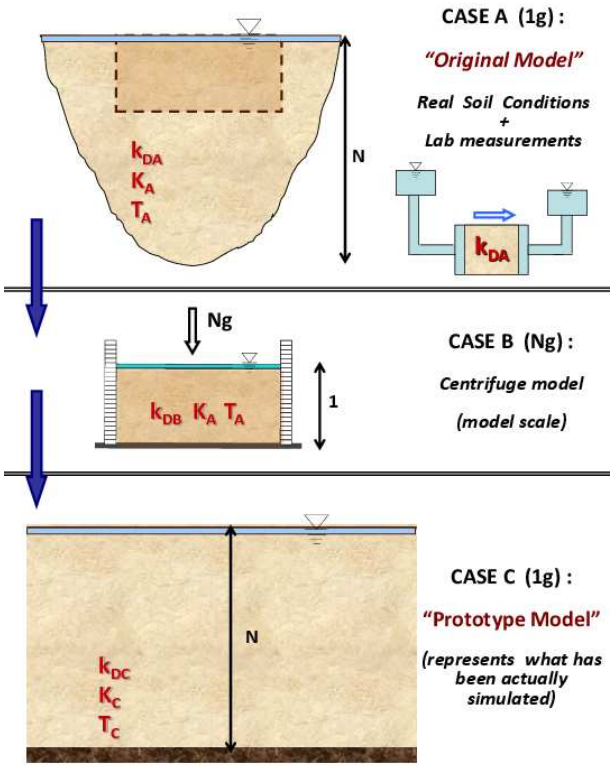

Figure 4: Schematic illustration of the centrifuge modeling concepts and scaling laws described in detail in Section 3.1. Case A represents the object for simulation, Case B represents the centrifuge model and Case C represents what has been actually simulated in prototype scale. The symbols, k_D, K and T, correspond to Darcy's permeability, specific permeability and consolidation time respectively.

Table 1: Scaling factors for a case of water filling the pore space (voids) in the soil.

	Case A	**Case B**	**Case C**
quantity	Original Model 1g	Centrifuge Model Ng Numerical Model 1	Prototype Model 1g Numerical Model 2
length	N	1	N
mass density	1	1	1
stress	1	1	1
strain	1	1	1
displacement	N	1	N
acceleration	$1/N$	1	$1/N$
Darcy's permeability	$1/N$	1	1
specific permeability	1	1	N
time (diffusion)	N^2	1	N
time (dynamic)	N	1	N
frequency	$1/N$	1	$1/N$

The base, to which all the scaling factors refer to, in Table 1, is the model scale. The column corresponding to the "Original Model" presents the scaling factors needed to be applied to the quantities in model scale in order to reproduce what has been intended to be simulated from the beginning -

the "Original Model". The conflict in time scales is related to the "Original Model". The column corresponding to the "Prototype Model" presents the scaling factors needed to be applied to the quantities in model scale in order to reproduce what has been actually simulated in prototype scale - the "Prototype Model" . Thus, comparison between what was intended to be studied (Case A) and what was studied in reality (Case C) can reveal scaling problems. A detailed analysis of scaling for each of three cases (A, B and C) follows.

Case A is the object for simulation and represents the prototype soil conditions and properties that are intended to be simulated through centrifuge modeling. Darcy's permeability, k_{DA}, of this type of soil has been measured in the lab. Case A could be simply described as a model N times larger than the centrifuge model with the same soil under 1g. The specific permeability, K_A and the time needed for completion of the 1D consolidation process, T_A, can be estimated using k_{DA} through Equation 1 and Equation 2 respectively.

$$K_A = \frac{k_{DA}}{\rho_f \times g} \tag{1}$$

$$T_A = \frac{H^2}{C_v} = \frac{H^2 \times \rho_f \times g}{k_{DA} \times E_{eod}} = \frac{H^2}{K_A \times E_{oed}} \tag{2}$$

Here ρ_f is the mass density of the fluid (water), g is the acceleration of gravity (9.81 m/s^2) in this case, H is the thickness of the soil layer in real/original scale and E_{oed} is the one dimensional soil stiffness:

Case B represents the centrifuge model which consists of the same type of soil as in case A with the same relative density. However, Darcy's permeability is proportional to the gravity, as it is indicated by Equation 1. The centrifuge gravity field (model) is $N \times g$, and the specific permeability, K, is a soil constant (independent of the permeant). It follows that by neglecting the changes of void ratio and the gravity level, the actual Darcy's permeability of the centrifuge model is N times larger that that of Case A, as shown in Equation 3 (Wood, 2004).

$$k_{DB} = K_B \times \rho_f \times N \times g = K_A \times \rho_f \times N \times g = N \times k_{DA} \tag{3}$$

Furthermore, the actual consolidation time of Case B becomes N^2 smaller than that of Case A, as shown in Equation 4.

$$T_B = \frac{(H/N)^2}{K_B \times E_{oed}} = \frac{H^2}{N^2 \times K_A \times E_{oed}} = \frac{T_A}{N^2} \tag{4}$$

In other words, the appropriate time scaling factor for the centrifuge measurements for diffusion is N^2, in order to get a similar response with Case A. On the other hand, the appropriate scaling factor for the dynamic time is N. This fact leads to a problem with realistic simulation of the Case A using centrifuge model. This stems from the fact that it is difficult to separate the dynamic and the diffusion times since they are both contributing to first rate physical effects and cannot be separated (both are of the same importance for liquefaction and cyclic mobility phenomena).

Case C represents what has been actually simulated and tested in (scaled up to) prototype scale, through the centrifuge modeling process. The centrifuge model under a gravity field of $N \times g$ corresponds to a soil layer N times larger in size in prototype scale, so that the stress field is common in both models.

Case C can be simply described as a model N times larger than the centrifuge model consisting of soil with the same Darcy permeability (N times less than that in Case A). Darcy's permeability of the prototype model (Case C) is equal to that of the centrifuge model (Case B), which means N times larger than that in Case A. Theoretically, the fact that $k_{DB} = k_{DC}$ leads to different values of specific permeability between the centrifuge model and the prototype one. In detail, the specific permeability of Case C, K_C, is N times larger than that of Case B and Case C, as described by Equation 5.

$$K_C = \frac{k_{DC}}{\rho_f \times g} = \frac{k_{DB}}{\rho_f \times g} = N \times K_B = N \times K_A \tag{5}$$

This is the recommended value of the specific permeability that should be used in numerical simulation of the centrifuge tests in prototype scale. Moreover, the diffusion time of the prototype model is estimated (Equation 6) to be N times less than that of the centrifuge model, which coincides with the scaling factor for the dynamic time.

$$T_C = \frac{H^2}{K_C \times E_{oed}} = \frac{H^2}{N \times K_B \times E_{oed}} = \frac{T_B}{N} = N \times T_A \tag{6}$$

However, the diffusion time of the prototype model is N times larger when compared to Case A.

Since the permeability is proportional to gravity, this presents a problem for modeling real scale case (Case A) using changed (larger) gravity field (Case B), if water is used as pore fluid.

Use of Higher Viscosity Replacements Fluids. In order to overcome this scaling discrepancy and achieve the same value of permeability in all cases, fluids with larger viscosity are chosen to fill the voids within the soil, according to Equation 7 below:

$$k_D = \frac{K \times \rho_f g}{\mu} \tag{7}$$

where μ is pore fluid viscosity. The Equations 8 and 9

$$k_{DA} = K \times \rho_w g \tag{8}$$

$$k_{DB} = \frac{K \times \rho_f \times N \times g}{\mu} \tag{9}$$

indicate that the pore fluid viscosity should be equal to $\rho_f \times N/\rho_w$, where ρ_w is the mass density of the water, so that $k_{DA} = k_{DB}$. In that case, the scaling factor for the diffusion time is equal to $\rho_f \times N/\rho_w$ instead of N^2 when water is used. In particular, if the pore fluid has the same mass density as water, then the time scaling factor for diffusion is the same as the one for dynamic events.

Wood (2004) suggests the use of silicone fluid as a replacement fluid. Another possibility is to use a solution of Hydroxypropyl methylcellulose in water, which, when mixed in right proportion, increases the viscosity of water from $1mm^2/s$ to approximately $25mm^2/s$ (Kulasingam et al., 2004). Increasing viscosity more than that amplifies the problem of proper (full) saturation of the sample, which than significantly affects other aspects of the experiment. By using scaled up viscosity of (up to) $\mu = 25mm^2/s$, the geometric scaling of model is also limited to 25. That means that any centrifuge experiment that uses $\mu = 25mm^2/s$ and is modeled in a centrifuge spinning at 50g level, using original soil, will have a scaling factor for the diffusion time equal to $25(1/50)^2/1 = 0.01 = 1/100$ and for the dynamic time equal to $(1/50)\sqrt{1/1} = 0.02 = 1/50$. That is, the geometric scaling will properly match the dynamic time scale while diffusion time scale will be half of what it is supposed to be. This means that the

diffusion is occurring twice as fast in comparison with the original model. Similarity of the original and the centrifuge model does not exist in this case. The larger the geometric scaling is, when compared to the fixed value of viscous scaling (usually not more than 25), the larger the discrepancy in time scale is. This inconsistency in scaling creates the so called distorted models as they inappropriately scale one of the first order phenomena.

3.2 Numerical Simulation of RPI Centrifuge Test (Model No1, Test 2) by Taboada and Dobry (1993)

Numerical modeling and simulation of the liquefaction is performed using the $u-p-U$ (Zienkiewicz and Shiomi, 1984; Jeremić et al., 2008) formulation in combination with the constitutive model by Dafalias and Manzari (2004). For validation, results from the centrifuge tests of Model No. 1 (test 2) presented by Taboada and Dobry (1993) from VELACS project are used.

A schematic configuration of the centrifuge model No.1 is illustrated in Figure 5. The soil consists of a uniform layer of Nevada sand with relative density $D_r \approx 40\%$ and is fully-saturated with the pore fluid. The thickness of the soil layer is 20 cm in model scale and the field of gravity applied to the model is 50g. The input motion applied to the base of the model is also shown in Figure 5 in real time (model) scale. According to the scaling laws provided by Wood (2004), the prototype model is 10 m thick and its Darcy permeability is 50 times greater than the value obtained from lab tests, as reported by Arulmoli et al. (1992). Accelerations, displacements and pore pressures were measured during testing at select locations. The locations and the type of measurements recorded are shown in Table 2.

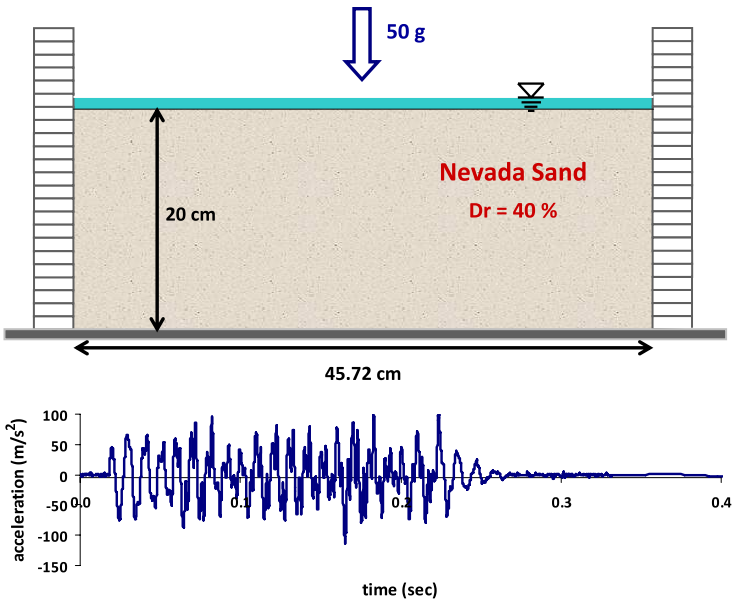

Figure 5: Schematic configuration of Model No. 1, Test 2, RPI (Taboada and Dobry, 1993).

Prior to the numerical simulation, calibration of SANISAND (Dafalias and Manzari, 2004) constitutive model was performed for Nevada sand, using soil data reported by Arulmoli et al. (1992) in the framework of VELACS project. Taiebat et al. (2010) present the values of the material parameters of SANISAND for Nevada sand, shown in Table 3. Fig. 6 compares the stress paths and stress-strain loops for Nevada sand with $D_r \approx 40\%$ obtained from lab tests with those obtained from calibration process.

After the calibration of the model, numerical simulation of direct shear test was conducted so as to find the relationship between the cyclic resistance of Nevada sand with relative density $D_r = 40\%$, versus the number of cycles to liquefaction, and compare it with the experimental data by Arulmoli

Table 2: Location and Type of Measurement in Model No. 1, Test 2, RPI

Measurement	Instrument ID	Depth in model scale	Depth in prototype scale
horizontal acceleration	$AH1$	$20cm$	$10m$
horizontal acceleration	$AH3$	$0cm$	$0m$
horizontal acceleration	$AH4$	$5.2cm$	$2.6m$
horizontal acceleration	$AH5$	$10cm$	$5m$
horizontal displacement	$LVDT3$	$0.9cm$	$0.45m$
horizontal displacement	$LVDT4$	$5cm$	$2.5m$
horizontal displacement	$LVDT5$	$10cm$	$5m$
horizontal displacement	$LVDT6$	$15cm$	$7.5m$
vertical displacement	$LVDT1$	$0cm$	$0m$
pore fluid pressures	$P1$	$2.9cm$	$1.45m$
pore fluid pressures	$P2$	$5.2cm$	$2.6m$
pore fluid pressures	$P3$	$10cm$	$5m$
pore fluid pressures	$P4$	$15cm$	$7.5m$

et al. (1992). The numerical model consisted of a single $u-p-U$ brick element subjected to cyclic horizontal shear loading under undrained conditions. Two different initial vertical effective stresses were considered, 20kPa and 70kPa, in order to investigate the effect of the initial confining stress, as captured by the model. The cyclic stress ratio, CSR, is defined as the ratio of horizontal shear stress to the initial vertical effective stress. The number of cycles to liquefaction both in the experiment and the analysis is determined according to the following criteria: (i) either the axial strain exceeds 1.5% or (ii) the excess pore water pressure ratio becomes equal to one. Figure 7 illustrates the comparison between the numerical and experimental data, showing, a fairly satisfactory agreement.

Most frequently, the numerical simulation of centrifuge tests is conducted in prototype scale. However, due to conflicts related to the appropriate scaling of dynamic time and dissipation-time, when water is used in tests (Wood (2004)), a different approach was adopted in the present study. Two different numerical models were used:

1. Numerical Model #1 in model scale.

   The numerical model #1 consists of a soil column of twenty 8-node $u-p-U$ brick elements with dimensions $1cm \times 1cm \times 1cm$. The total height of the soil column is 20 cm. The gravity applied to the model is equal to 50g. The input motion is shown in Fig. 5. The specific permeability, K, is $3.2 \times 10^{-6} cm^3 s/g$. The results of the analysis are illustrated in Fig. 8 and 9 in model scale in terms of time histories of displacements and accelerations respectively.

2. Numerical Model #2 in prototype scale.

   The numerical model #2 consists of a soil column of twenty 8-node u-p-U brick elements with dimensions $0.5m \times 0.5m \times 0.5m$. The total thickness of the soil column is 10 m. The gravity

Table 3: Material parameters of Dafalias-Manzari model.

Material Parameter		**Value**	**Material Parameter**		**Value**
Elasticity	G_0	150 kPa	Plastic modulus	h_0	9.7
	v	0.05		c_h	1.03
Critical sate	M	1.14		n_b	2.56
	c	0.78	Dilatancy	A_0	0.81
	λ_c	0.027		n_d	1.05
	ξ	0.45	Fabric-dilatancy	z_{max}	5.0
	e_r	0.83		c_z	800.0
Yield surface	m	0.05			

applied to the model is equal to 1g. The input motion has been modified to prototype scale (the dynamic time has been multiplied by 50 and the acceleration has been divided by 50). The specific permeability, K, is $1.6 \times 10^{-4} cm^3 s/g$. The results of the analysis are illustrated in Figs. 10 to 15. Results are presented in prototype scale and are comparing Numerical Models #1 and #2 after scaling laws between Case B and C of Table 1 were applied - apart from strain and stresses which are in the same scale by default for both models.

The soil properties used for the both numerical models are shown in Table 4. The Newmark time integration method is used since it was shown in verification study (Tasiopoulou et al., 2014) to better dissipate high frequencies introduced in the coupled system by the discretization process. The Newmark parameters used for all the numerical analysis for both models are: $\gamma = 0.7$, $\beta = 0.42$. The column is horizontally excited during a second stage of loading, after first stage self-weight loading. It should be noted that the self weight loading is performed on an initially zero stress (unloaded) soil column and that the material model and constitutive integration algorithm is versatile enough to follow through this early loading with proper parameter evolution. The boundary conditions are such that the soil and water displacement degrees at the bottom surface are fixed, the pore fluid pressure degrees are free; the soil and water displacement degrees at the upper surface are free, however the pore pressure degrees are fixed (zero pore fluid pressure) to simulate the upward drainage. In order to simulate one dimensional shaking (shear box), all the degrees of freedom at the same level are constrained in a master-slave fashion.

The Darcy permeability of Nevada sand with $D_r \approx 40\%$, varies in the range of $k_D = 2.1 \times 10^{-5} m/s$ to $k_D = 3.3 \times 10^{-5} m/s$, as reported by Arulmoli et al. (1992). The prototype model is considered to have 50 times larger Darcy permeability that the one measured in the lab. The Darcy permeability used in the present study for both Numerical Models #1 and #2 is $1.6 \times 10^{-3} m/s$. It is noted that the input parameter in our numerical code is the specific permeability, K, given by Equation 10:

$$k = \frac{k_D}{\rho_f \times G} \tag{10}$$

where G is equal to 50g for Numerical Model #1 and 1g for Numerical Model #2.

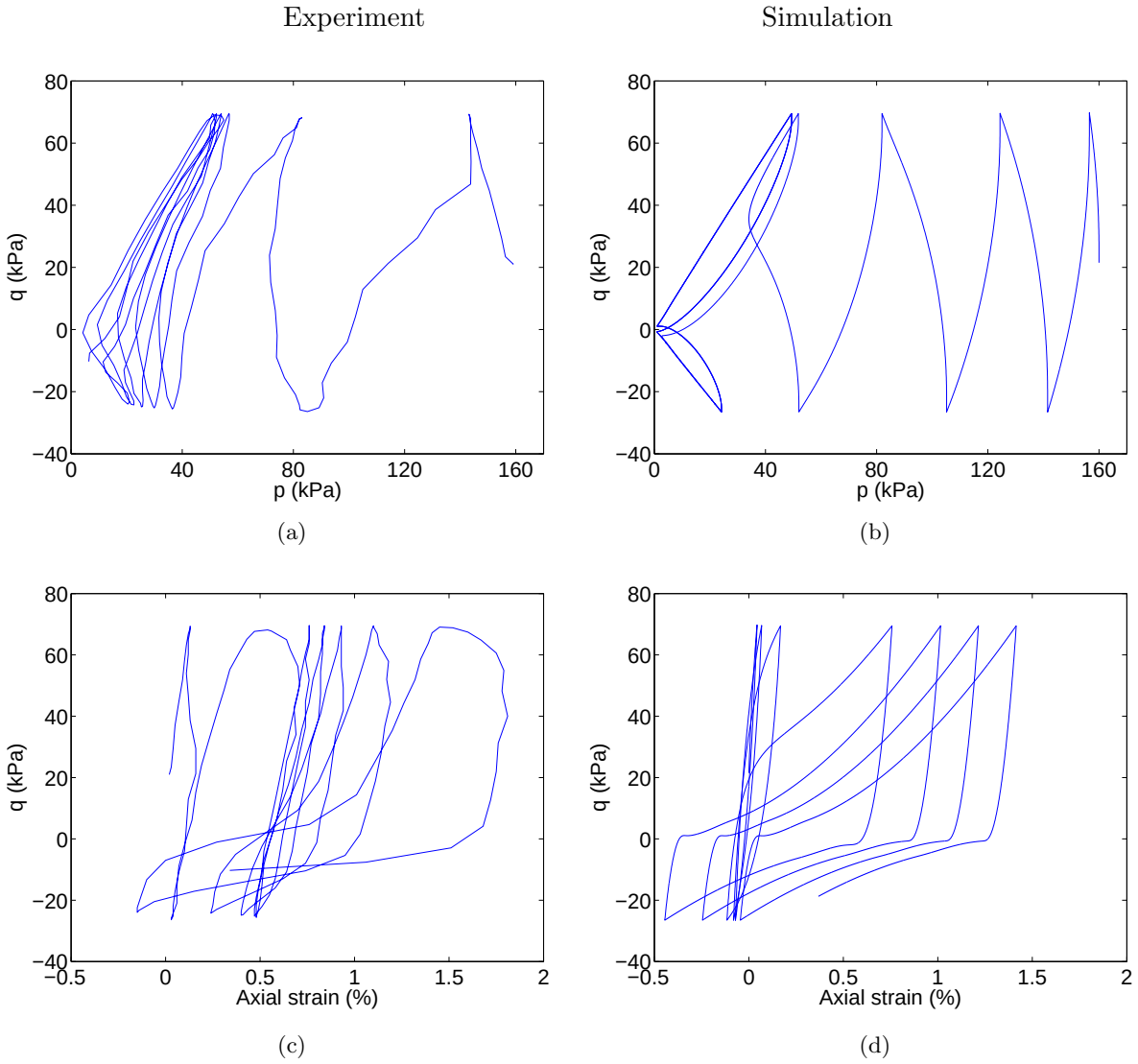

Figure 6: Simulations versus experiments in undrained triaxial tests on Nevada sand with $D_r \approx 40\%$ published by Taiebat et al. (2010). The experimental data can be found in Arulmoli et al. (1992).

3.3 Discussion of Numerical Results

Comparison between Numerical Model #1 and Numerical Model #2. The results obtained from the Numerical Model #1 are shown in Figures 8 to 9 in model scale in order to illustrate that this type of analysis, using very small size of elements and time step can be easily performed by the numerical code and also to illustrate/present results that are obtained in model scale in a centrifuge experiment. The numerical results obtained from Numerical Model #1 were scaled to prototype scale according to the scaling laws (Table, 1 between Column 2 and 3), so that they can compared with those of Numerical Model #2.

This comparison between Numerical Models #1 and #2, illustrated in Figures 10 to 15, is used to verify the scaling factors derived in section 3.1, while also giving a better insight in the intrinsic differences that occur due to the difference in scale of the two numerical models.

Numerical results between the two models compare well for displacements, accelerations and excess pore water pressure. In particular, Figure 12 shows a complete agreement of the numerical results in the dissipation of the excess pore pressure during and after the end of shaking. Here the excess pore water

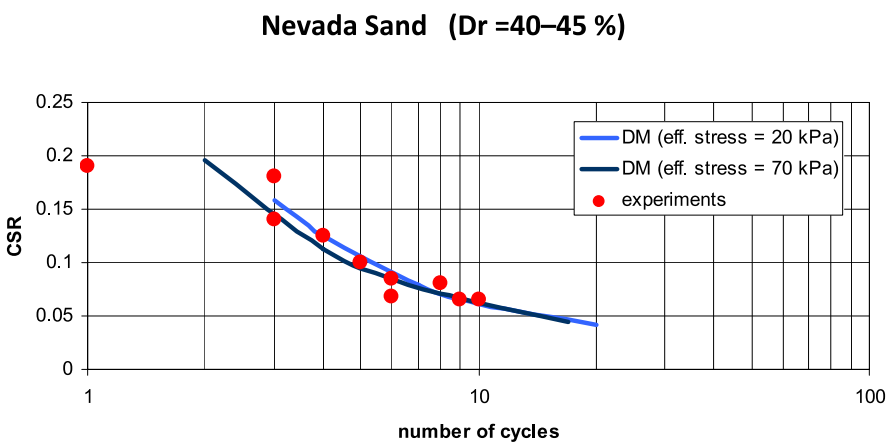

Figure 7: Cyclic shear stress ratio for Nevada sand with relative density $D_r = 40 - 45\%$ versus the number of cycles to liquefaction. Comparison between the numerical results using material model from Dafalias and Manzari (2004) and the experimental data by Arulmoli et al. (1992).

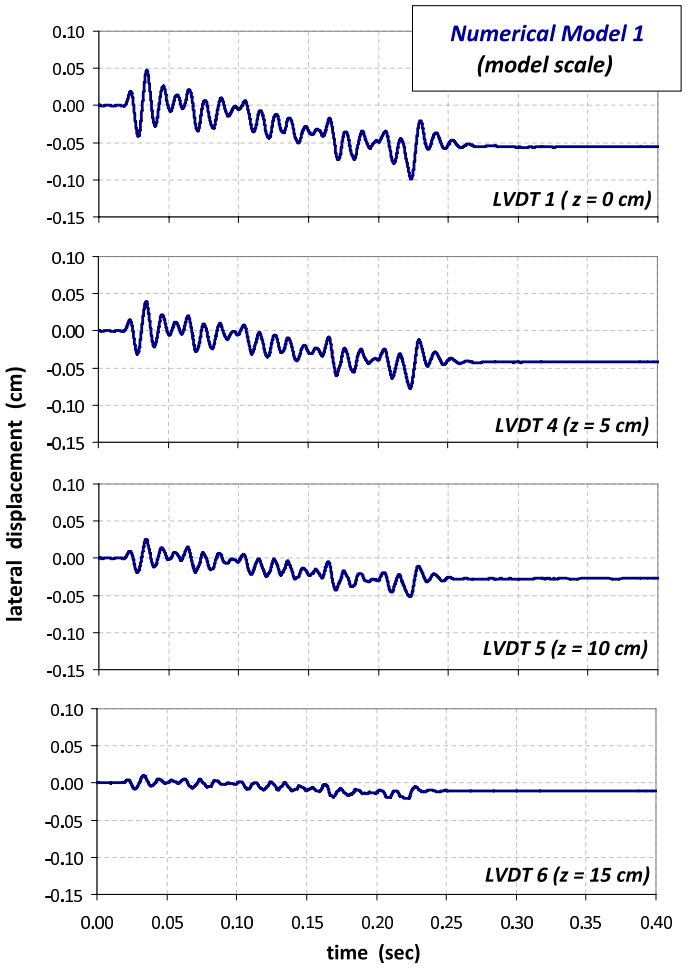

Figure 8: Time histories of horizontal displacements at the depths of 0, 5 ,10 and 20 cm from the surface in model scale, as obtained from Numerical Model 1.

pressure, r_u, is defined as the ratio of excess pore water pressure over the initial vertical effective stress. The slight difference in the results, shown in time histories of displacement (Figure 10) is resulting from

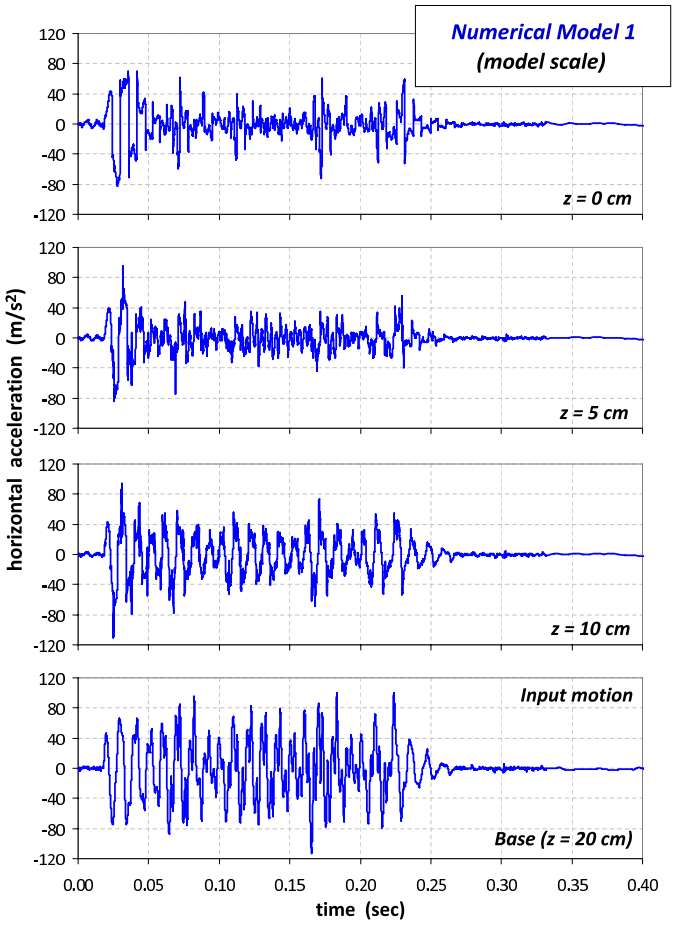

Figure 9: Time histories of horizontal acceleration at the depths of 0, 5 ,10 and 20 cm from the surface in model scale, as obtained from Numerical Model 1.

Table 4: Soil Properties for the centrifuge test, Model No. 1, test 2, RPI

Parameter	Symbol	Value
gravity acceleration	g	9.81 m/s^2
solid particle density	ρ_s	2.65×10^3 kg/m^3
water density	ρ_f	1.0×10^3 kg/m^3
solid particle bulk modulus	K_s	36.0×10^6 kN/m^2
fluid bulk modulus	K_f	2.2×10^6 kN/m^2
porosity	n	0.4253
initial void ratio	e_0	0.74
Darcy permeability	k_D	1.6×10^{-3}m/s
Biot coefficient	α	1.0

differences in the stress paths and stress-strain loops shown in Figures 14 and 15 respectively. Numerical Model #1 demonstrates a more dilative behavior giving larger negative strains than Numerical Model

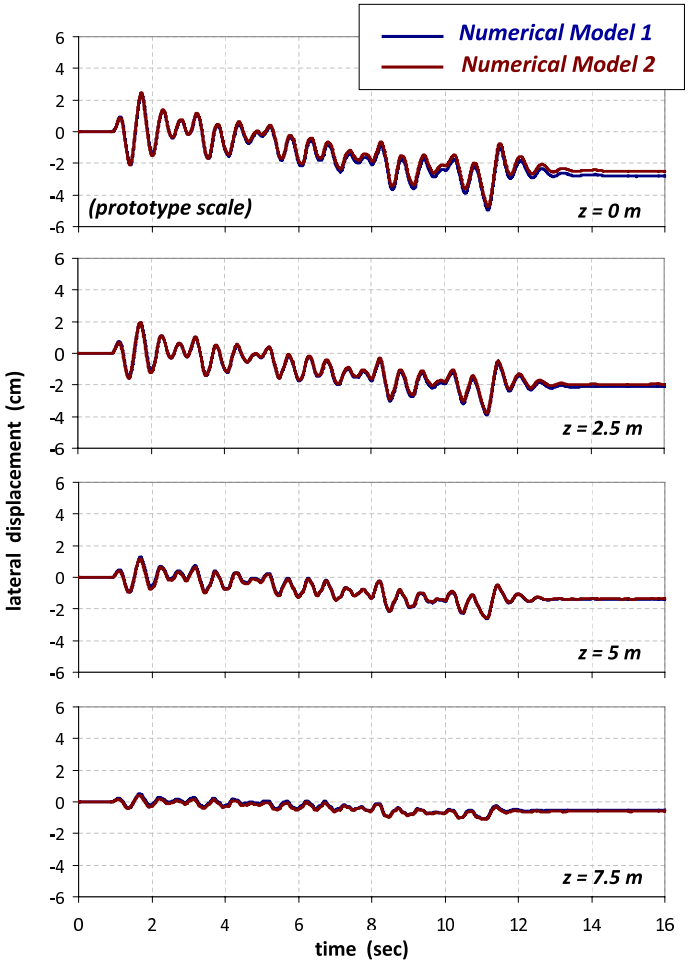

Figure 10: Time histories of horizontal displacement at the depths 0, 2.5, 5, 7.5 m from the surface. Comparison between the results obtained from Numerical Model 1 and Numerical Model 2, in prototype scale.

#2. These differences are related to the velocity proportional damping associated with the $u-p-U$ formulation. Velocity proportional damping is related to permeability (Jeremić et al., 2008), and in this particular case, it is related to intrinsic permeability which does not scale. As discussed by Tasiopoulou et al. (2014), intrinsic (isotropic) permeability k has dimensions of $[L^3TM^{-1}]$ and is different from Darcy permeability (hydraulic conductivity), (k_D), which has the dimension of velocity, i.e. $[LT^{-1}]$. They are related by $k = k_D/g\rho_f$, where g is the gravitational acceleration and ρ_f is the density of the pore fluid which is slightly changed here. However, effects are small and are mostly apparent at lower levels of the centrifuge model. It should be noted that there are two types of energy dissipation in fully-coupled systems: (i) velocity proportional damping due to viscous coupling and (ii) displacement proportional damping due to frictional damping and elasto-plasticity (Argyris and Mlejnek, 1991). In this case displacement proportional damping (energy dissipation) related to elasto-plasticity is much larger than velocity proportional damping, and controls the response.

Figure 14, shows the reduction of the vertical effective stress as a function of cyclic shear stress. It is also noted that vertical effective stress rebounds after shaking stops. The r_u time histories in Figure 12 give clearer effective stress reduction and rebounding. We define that liquefaction occurred for values of $r_u \geq 0.90$. It is also apparent (Figure 15) that the shear modulus decreases as the shaking progresses and the pore fluid pressure increases. It is important to note that not all soil layers experience liquefaction, as r_u decreases with the depth increase. The excess pore fluid pressure dissipation at the lower layers is

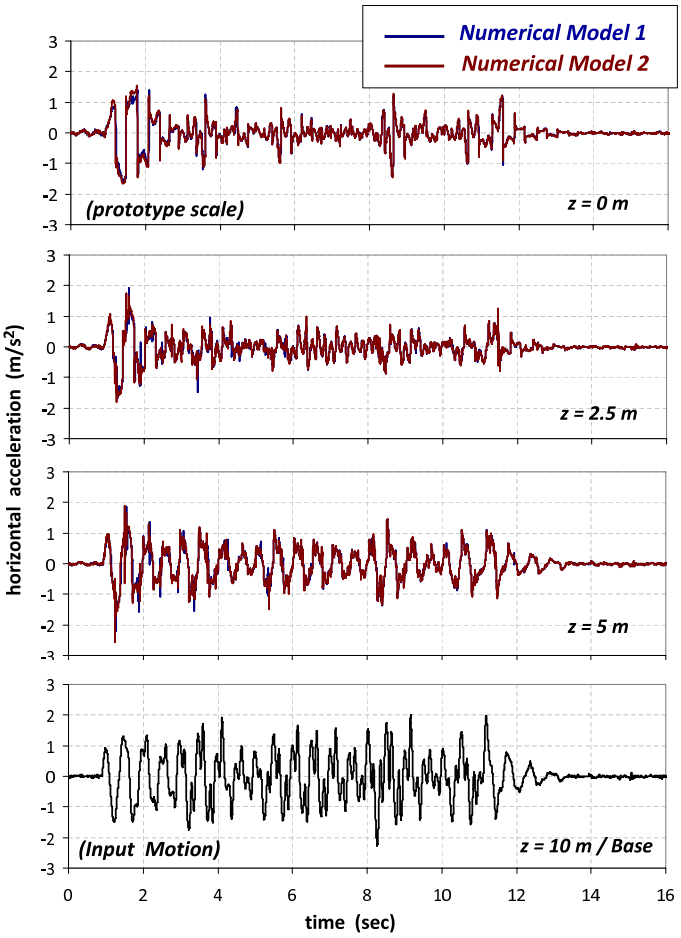

Figure 11: Time histories of horizontal acceleration at the depths 0, 2.5, 5, 10 m from the surface. Comparison between the results obtained from Numerical Model 1 and Numerical Model 2, in prototype scale.

quicker than that of the upper layers. The upper layers have to dissipate their own excess pore pressure, however they also receive additional volume of water from lower levels (dissipation is upward). This leads to increase in pore fluid pressure at top layers even after the shaking has stopped (see upper three plots in Figure 12). The soil settlement and water drainage continue after the initial shaking is over mainly due to the continuous pore fluid movement upward.

Comparison between numerical and centrifuge results. The comparison of the numerical and the centrifuge results are presented in Figures 16 to 18. The time and displacements are multiplied by 50 and the accelerations are divided by 50, according to the scaling laws provided in section 3.1. Scaled results are validated using centrifuge results, as presented by Taboada and Dobry (1993).

In general, it is shown that the physical mechanism of liquefaction is captured by the numerical analysis, providing validation of numerical modeling. In particular, the displacement time histories, and especially the residual values of displacement (see Fig. 16) indicate good agreement with the experimental results. The magnitude of cyclic component, however, is underestimated by the numerical results, a phenomena which was also observed in other studies (Elgamal et al., 2002; Taiebat et al., 2007). The excess pore pressure time histories (Fig. 18) indicate good agreement between numerical and centrifuge results, except for the deepest layer. Earlier rise in excess pore pressures is observed in the numerical analysis when compared to the centrifuge test. Differences in liquefaction initiation and timing affect

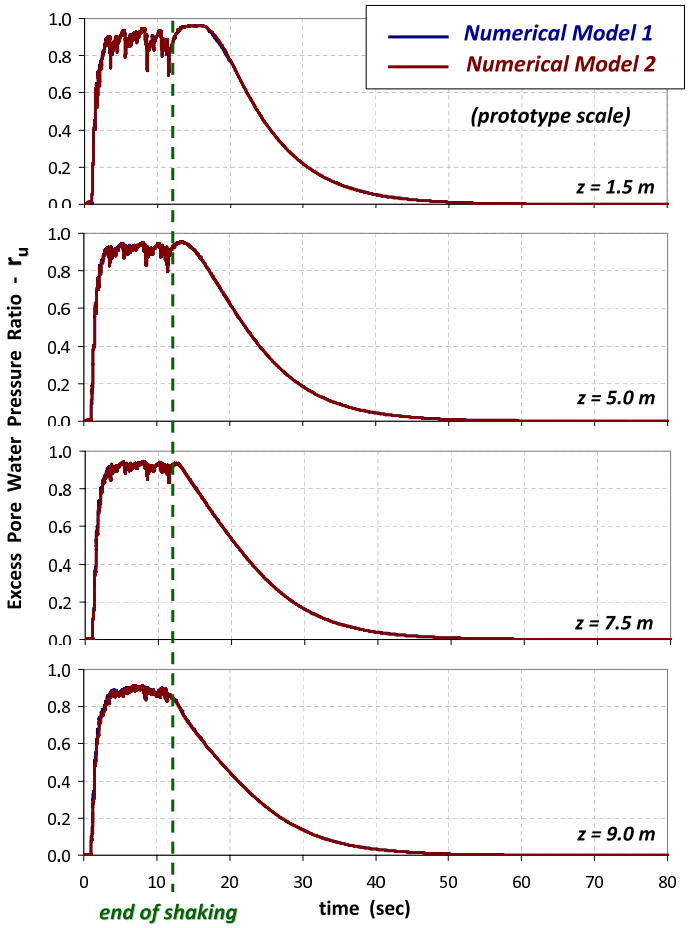

Figure 12: Time histories of excess pore water pressure at the depths 1.5, 5, 7.5, 9 m from the surface. Comparison between the results obtained from Numerical Model 1 and Numerical Model 2, in prototype scale.

the acceleration time histories, as can be observed in Fig. 17. The cut-off of acceleration, indicative of liquefaction[3], start to occur deep in the soil column (location AH5), and this contrasts the experimental results. These results are compatible with the development of excess pore pressure shown in Figure 18. However, there is a good agreement between the numerical and the centrifuge results in terms of the acceleration time history at the surface of the soil layer.

The fact that liquefaction seems to occur deep in the soil column for the numerical case, may be attributed to the calibration of the constitutive model. By observing the stress paths in Figs. 14 and 15, it can be noted that there is a quick decrease of the effective vertical stress at all depths. This may be attributed to the fact that the current constitutive model is based only on changes in stress ratio (see Figure 7) , whereas in reality the rate of excess pore pressure generation depends on the initial mean effective stress as well. This could be modified by adjusting the values of the parameters of the model with depth in order to capture this specific case. However, the intention of this study is to calibrate the constitutive model using the soil data obtained from laboratory (triaxial) tests, conducted in the framework of a VELACS project, and thus perform a real numerical prediction of behavior observed in physical tests, without using centrifuge test results to (back/re-) calibrate (change) material parameters. This approach contrasts an approach (often used) in which material model parameters are re-calibrated (changed) so that numerical results fit the centrifuge test data, while neglecting prior calibration from

[3]and providing for base isolation by liquefaction, as described by Taiebat et al. (2010).

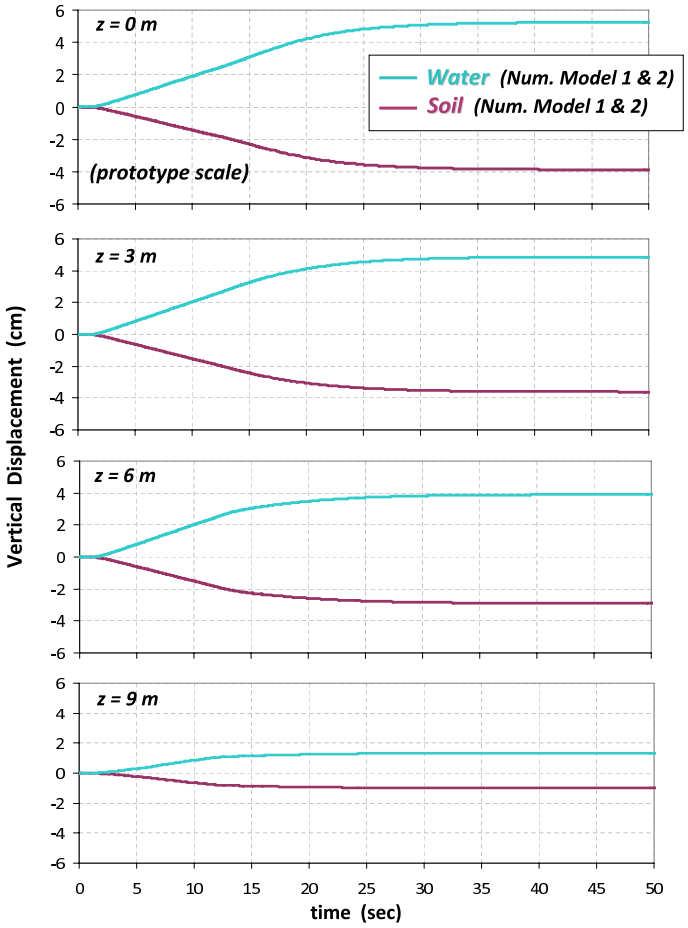

Figure 13: Time histories of vertical displacement at the depths 0, 3, 6, 9 m from the surface. Comparison between the vertical outward movement of the water and the settlement of the soil, in prototype scale.

laboratory (triaxial) tests. Possible improvement to the material model would be to render some parameters of the constitutive model dependent on the confining stress, for example the parameters that control the dilatancy, such as A_d.

Comparison of vertical displacements, shown in Figure 19, shows again differences in magnitude. These differences are significant and have been occasionally reported in technical meetings, but to our knowledge, have never been presented or published in an archival journal.

There are a number possible effects that can be used to explain the observed discrepancies between the numerical and centrifuge results.

3.4 Comments on Validation Testing Using Centrifuge Modeling Results

Provided here are comments related to potential issues with our numerical modeling and with centrifuge modeling results use for validation of numerical modeling and simulation.

Use of Constant Permeability. Permeability of soil changes during liquefaction (Shahir et al., 2012). However, the effect of changing permeability is not modeled in this study. This modeling simplification can potentially have large effects on results, as with an increase in permeability during liquefaction, water moves more freely and thus more settlement occurs.

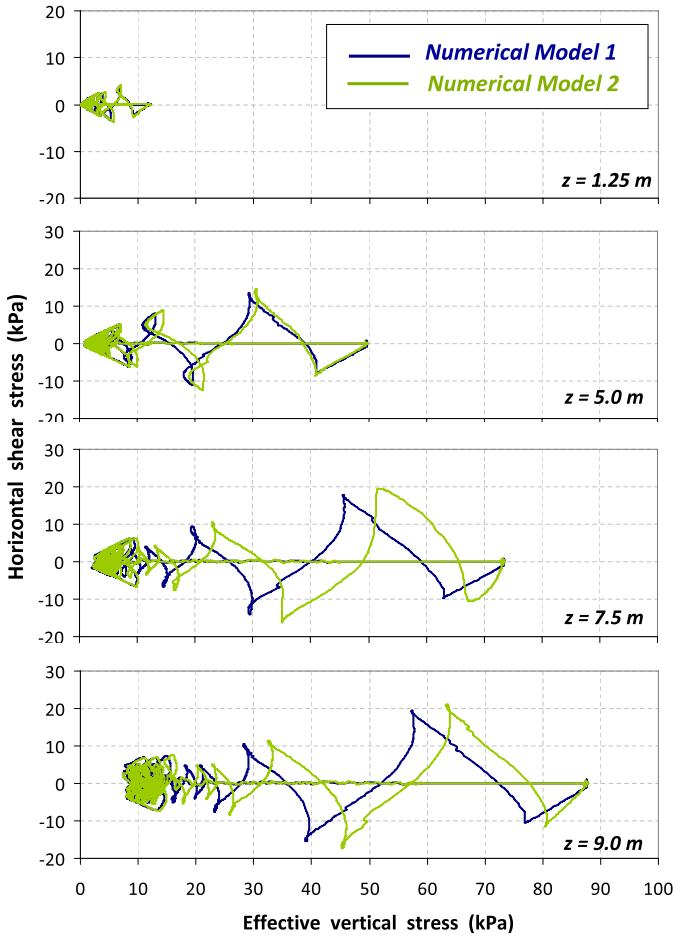

Figure 14: Horizontal shear stress versus effective vertical stress at the depths of 1.25, 5, 7.5, 9 m. Comparison between the stress paths obtained from Numerical model 1 and Numerical Model 2.

Boundary Conditions. Idealized boundary conditions used in numerical simulation of centrifuge experiments simulate a 1D shear beam. These boundary conditions mimic a laminar box around the contained soil. For numerical model, these boundary conditions allow the (separate) vertical movement of the soil and water (while allowing horizontal shaking of soil and water) and prevent any lateral expansion. However, the real conditions in the centrifuge model involve 3D effects that, for example, may allow for a lateral flow and consequently quicker dissipation which leads to slower built up of excess pore pressures. While we know that full 3D behavior is present in a centrifuge laminar box, limitations in instrumentation and pre-assumption of 1D behavior leave us with no data (measurements) of such 3D behavior. The only options thus is to numerically model a 1D shear box.

Variability of Material in Laboratory Test and Centrifuge Model. Laboratory tests performed on same (similar) soil were used for calibration of material model that was then used in modeling and simulation validation, using centrifuge tests. It is not clear how similar soil used in those laboratory tests is to the soil used in a centrifuge experiment. Only relative density is used to describe both soils (same Nevada sand), however, other factors do affect soil behavior. For example, sand fabric and anisotropy, both initial and induced, have certainly been different for laboratory and centrifuge tests, and yet information about those differences is not available (not measured). Differences in material behavior can significantly affect the final numerical simulation and test results, and that might be one of the reasons for some of the discrepancies in this validation study.

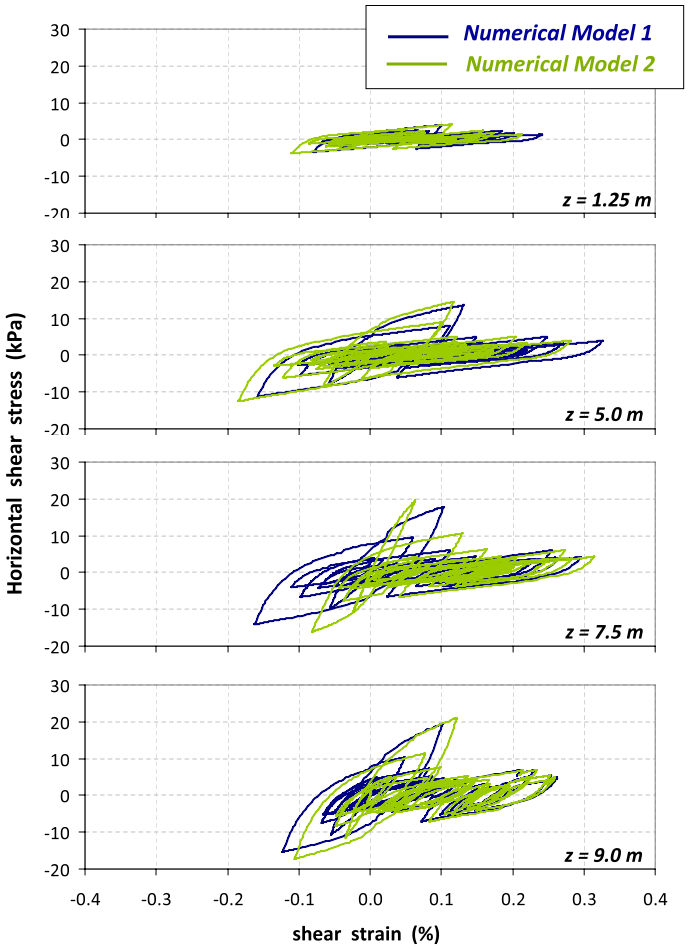

Figure 15: Shear stress-strain loops at the depths of 1.25, 5, 7.5, 9 m. Comparison between the stress paths obtained from Numerical model 1 and Numerical Model 2.

Scaling of Dynamic and Dissipation Time. It is common to perform numerical modeling of centrifuge tests in prototype scale. This is due to the fact that centrifuge results are published in prototype scale, while, unfortunately, the scaling factors that have been used are not always reported. Scaling factors used to present the experimental measurements in prototype scale correspond to Case C (see Table 1), resulting in similarity of diffusion and dynamic time. These are the scaling factors applied to the current study. However, the scaling relationships were not enforced in the centrifuge. This can lead to a possible concussion that since diffusion happens faster than pore water pressure generation, more diffuses that is the reason for slower pore fluid pressure rises and larger settlements in centrifuge.

Scaling of Failure Zones – Shear Bands. Scaling problems for failure of soils, where localization of deformation occurs, can bring additional challenges. Sand (coarse grained particulate material) develop shear zone that is usually 5-20 sand particles wide (Alshibli and Sture, 2000). That means that if model and original soil are the same, i.e. Nevada sand with mean grain size of 0.15 mm, the original shear zone width will be between $5 \times 0.15\text{mm} = 0.75\text{mm}$ and $20 \times 0.15\text{mm} = 3.00\text{mm}$ wide, while the same width of shear zone will be carried to the model scale. Ideally, in model scale the shear zone would have to be scaled down N times, which is not the case here. This can have effect on any phenomena modeled in centrifuge where localized deformation occurs, as for example is the case of vertically propagating shear waves, which plastify (and fail) soil as they propagate. This lack of scaling of the plastified/shear band zone can influence results, particularly when soil in such shear zone dilates and compresses, while pore

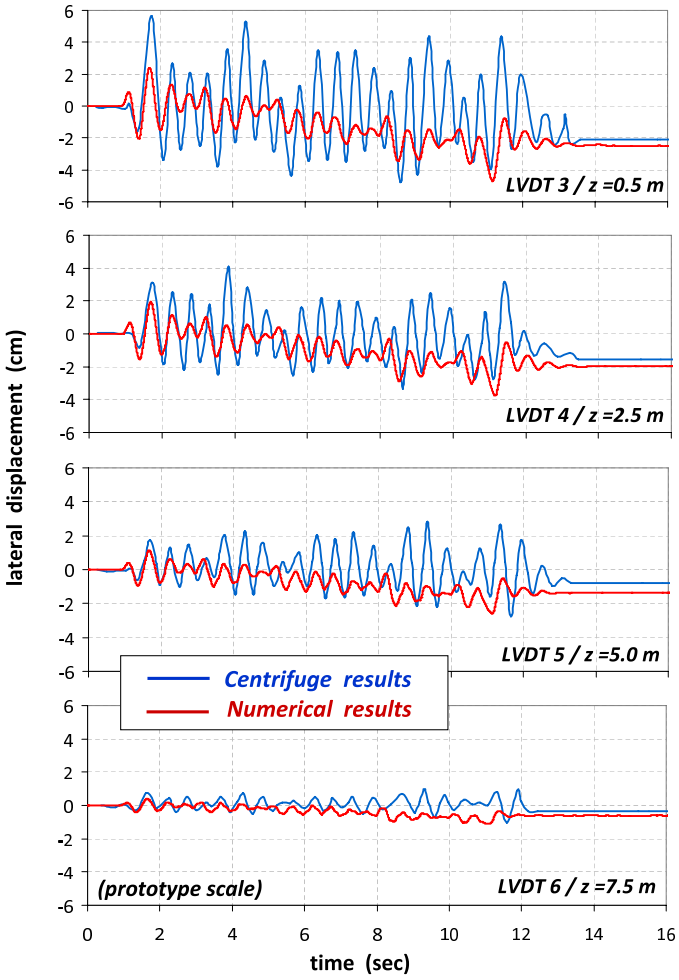

Figure 16: Time histories of horizontal displacements at the locations LVTD3, LVDT4, LVDT5 and LVDT6. Comparison between the numerical and the experimental results from the centrifuge test, in prototype scale.

fluid is being pumped out and in.

Uncertainty in Measurement Locations. The accuracy of location of measurements in the centrifuge can be ambiguous. For example, if the location of the instrumentation is off by 1 cm in the centrifuge model, this error translates to half a meter location error for a centrifuge experiment performed at 50g level. In addition, dense instrumentation and connecting wires within centrifuge model affect behavior of soils, but are not explicitly taken into account for validation.

4 Conclusions

Presented here was a validation study that aimed to validate numerical modeling and simulation of fully coupled behavior of fully saturated sand, using u-p-U formulation. Numerical models of centrifuge tests were used for validation. An extensive discussion of scaling laws as they apply to validation of numerical modeling using centrifuge test data was provided.

Numerical modeling was, for the most part, successfully validated. Observed differences have been explained using scaling laws, mechanics of coupled systems, and inconsistencies in boundary conditions (assumed versus actual). It is noted that centrifuge modeling can be very useful in modeling of coupled

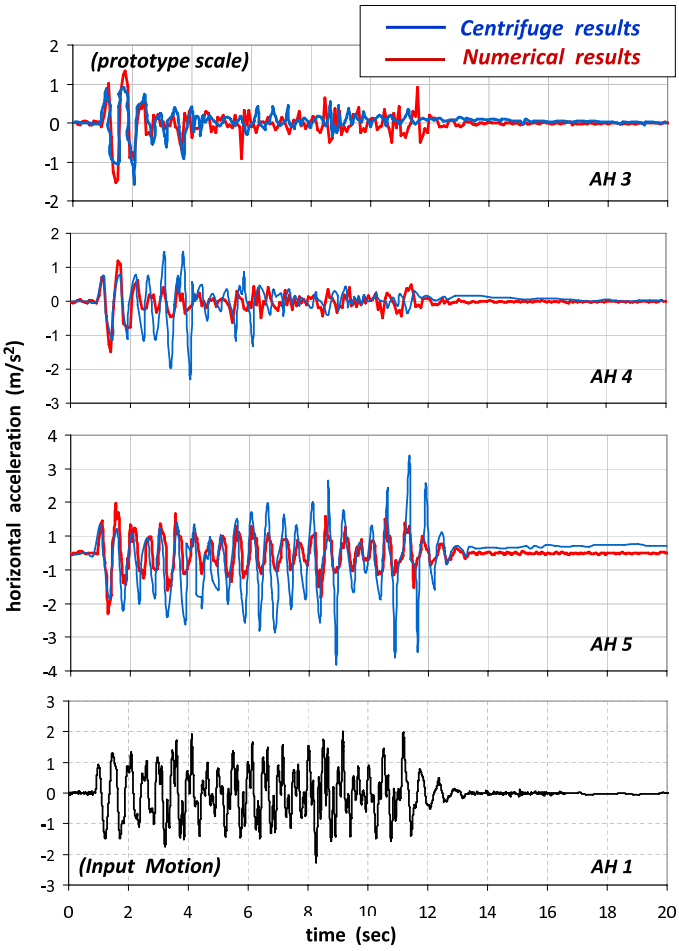

Figure 17: Time histories of horizontal accelerations at the locations AH1, AH3, AH4 and AH5. Comparison between the numerical and the experimental results from the centrifuge test, in prototype scale.

system, provided that scaling laws are carefully taken into account and that phenomena of first and second order importance are prioritized and separated.

On of the main conclusions is that numerical modeling and simulation can be successfully used to predict behavior of fully coupled solids (saturated soil) and thus used to improve design (safety and economy), provided that there is a clear trail of verification and validation for the numerical tool used. Without such documented verification and validation, software errors and modeling uncertainty that are (potentially) present in numerical modeling tools, can render results unreliable and thus unusable for design.

5 Acknowledgement

Author's would like to thanks Professor Bruce Kutter for many useful comments and guidance provided during this research.

References

K. Alshibli and S. Sture. Shear band formation in plane strain experiments of sand. *ASCE Journal of Geotechnical and Geoenvironmental Engineering*, 126(6):495–503, 2000.

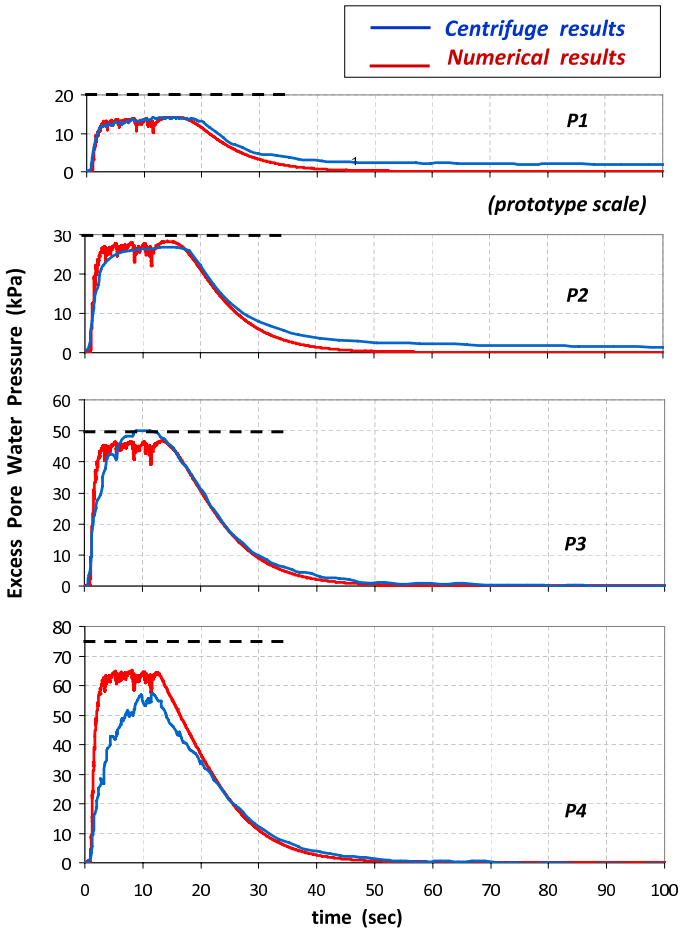

Figure 18: Time histories of excess pore water pressure at the locations P1, P2, P3 and P4. Comparison between the numerical and the experimental results from the centrifuge test, in prototype scale.

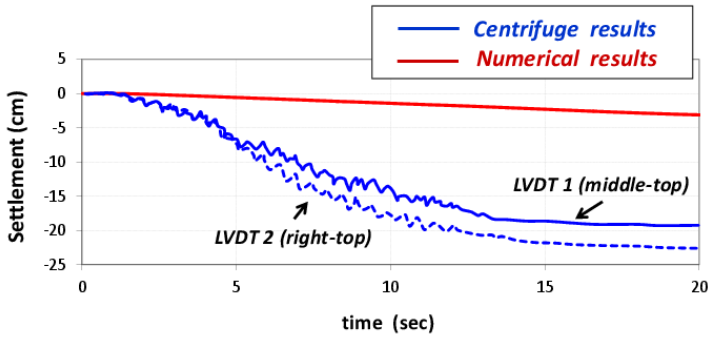

Figure 19: Time histories of vertical displacements (settlement). Comparison between the numerical and the experimental results (at two surface locations, middle – LVDT1 and quarter width from the side – LVDT2) from the centrifuge test, in prototype scale.

J. Argyris and H.-P. Mlejnek. *Dynamics of Structures.* North Holland in USA Elsevier, 1991.

K. Arulanandan and R. F. Scott, editors. *Verification of Numerical Procedures for the Analysis of Soil Liquefaction Problems.* A. A. Balkema, 1993.

K. Arulmoli, K. K. Muraleetharan, M. M. Hossain, and L. S. Fruth. Velacs: Verification of liquefaction

analyses by centrifuge studies - laboratory testing program. soil data report. Technical report, Earth Technology Corporation, 1992.

I. Babuška and J. T. Oden. Verification and validation in computational engineering and science: basic concepts. *Computer Methods in Applied Mechanics and Engineering*, 193(36-38):4057–4066, Sept 2004.

J. Bielak, R. W. Graves, K. B. Olsen, R. Taborda, L. Ramírez-Guzmán, S. M. Day, G. P. Ely, D. Roten, T. H. Jordan, P. J. Maechling, J. Urbanic, Y. Cui, and G. Juve. The shakeout earthquake scenario: Verification of three simulation sets. *Geophysical Journal International*, 180(1):375–404, 2010. ISSN 1365-246X. doi: 10.1111/j.1365-246X.2009.04417.x. URL `http://dx.doi.org/10.1111/j.1365-246X.2009.04417.x`.

Y. F. Dafalias and M. T. Manzari. Simple plasticity sand model accounting for fabric change effects. *ASCE Journal of Engineering Mechanics*, 130(6):622–634, June 2004.

A. Elgamal, Z. Yang, and E. Parra. Computational modeling of cyclic mobility and post–liquefaction site response. *Soil Dynamics and Earthquake Engineering*, 22:259–271, 2002.

W. Heisenberg. Über den anschaulichen inhalt der quantentheoretischen kinematik und mechanik. *Zeitschrift für Physik*, 43:172–198, 1927. English translatation: J. A. Wheeler and H. Zurek, Quantum Theory and Measurement, Princeton Univ. Press, 1983, pp. 62-84.

B. Jeremić, Z. Cheng, M. Taiebat, and Y. F. Dafalias. Numerical simulation of fully saturated porous materials. *International Journal for Numerical and Analytical Methods in Geomechanics*, 32(13):1635–1660, 2008.

R. Kulasingam, E. J. Malvick, R. W. Boulanger, and B. L. Kutter. Strength loss and localization at silt interlayers in slopes of liquefied sand. *ASCE Journal of Geotechnical and Geoenvironmental Engineering*, 130(11):1192–1202, November 2004.

Z. Mróz. On proper selection of identification and verification tests. In A. Saada and G. Bianchini, editors, *Constitutive Equations for Granular Non–Cohesive Soils*, pages 721–722. A. A. Balkema, July 1988.

W. L. Oberkampf and C. J. Roy. *Verification and Validation in Scientific Computing*. Cambridge University Press, 2010. ISBN 978-0-521-11360-1.

W. L. Oberkampf, T. G. Trucano, and C. Hirsch. Verification, validation and predictive capability in computational engineering and physics. In *Proceedings of the Foundations for Verification and Validation on the 21st Century Workshop*, pages 1–74, Laurel, Maryland, October 22-23 2002. Johns Hopkins University / Applied Physics Laboratory.

J. T. Oden, I. Babuška, F. Nobile, Y. Feng, and R. Tempone. Theory and methodology for estimation and control of errors due to modeling, approximation, and uncertainty. *Computer Methods in Applied Mechanics and Engineering*, 194(2-5):195–204, February 2005.

T. Oden, R. Moser, and O. Ghattas. Computer predictions with quantified uncertainty, part i. *SIAM News,*, 43(9), November 2010a.

T. Oden, R. Moser, and O. Ghattas. Computer predictions with quantified uncertainty, part ii. *SIAM News,*, 43(10), December 2010b.

P. J. Roache. *Verification and Validation in Computational Science and Engineering*. Hermosa Publishers, Albuquerque, New Mexico, 1998. ISBN 0-913478-08-3.

C. J. Roy and W. L. Oberkampf. A comprehensive framework for verification, validation, and uncertainty quantification in scientific computing. *Computer Methods in Applied Mechanics and Engineering*, 200 (25-28):2131 – 2144, 2011. ISSN 0045-7825. doi: 10.1016/j.cma.2011.03.016. URL `http://www.sciencedirect.com/science/article/pii/S0045782511001290`.

H. Shahir, A. Pak, M. Taiebat, and B. Jeremić. Evaluation of variation of permeability in liquefiable soil under earthquake loading. *Computers and Geotechnics*, 40:74–88, 2012.

V. M. Taboada and R. Dobry. Experimental results of model no. 1 at rpi. In *Verification of numerical procedures for the analysis of soil liquefaction problems*, pages 3–18, Rotterdam: AA Balkema, 1993.

M. Taiebat, H. Shahir, and A. Pak. Study of pore pressure variation during liquefaction using two constitutive models for sand. *Soil Dynamics and Earthquake Engineering*, 27:60–72, 2007.

M. Taiebat, B. Jeremić, Y. F. Dafalias, A. M. Kaynia, and Z. Cheng. Propagation of seismic waves through liquefied soils. *Soil Dynamics and Earthquake Engineering*, 30(4):236–257, 2010.

P. Tasiopoulou, M. Taiebat, N. Tafazzoli, and B. Jeremić. Solution verification procedures for modeling and simulation of fully coupled porous media: Static and dynamic behavior. *Coupled Systems Mechanics Journal*, In Review, 2014.

D. M. Wood. *Geotechnical Modeling*. Spoon Press, 2004. ISBN 0-415–34304.

O. C. Zienkiewicz and T. Shiomi. Dynamic behaviour of saturated porous media; the generalized Biot formulation and its numerical solution. *International Journal for Numerical and Analytical Methods in Geomechanics*, 8:71–96, 1984.

O. C. Zienkiewicz, M. Huang, and M. Pastor. Numerical modelling of soil liquefaction and similar phenomena in earthquake engineering: State of the art. In K. Arulanandan and R. F. Scott, editors, *Verification of Numerical Procedures for the Analysis of Soil Liquefaction Problems*, volume 2, pages 1401–1414, 1994.